Pergamon

Int. J. Heat Mass Transfer. Vol. 38, No. 18, pp. 3349–3358, 1995

0017–9310/95 $9.50+0.00

0017–9310(95)00102–6

Theoretical and experimental investigation of a constant-pressure adsorption process

A. HAJJI and S. KHALLOUFI

Département de Génie Industriel Alimentaire, Institut Agronomique et Vétérinaire Hassan II, B.P. 6202 Rabat-Instituts, Morocco

(*Received* 23 *September* 1994 *and in final form* 17 *February* 1995)

Abstract—This paper presents a theoretical and experimental analysis of a constant pressure adsorption process. The governing heat and mass transfer equations derived from local thermodynamic equilibrium and energy balance are solved numerically. The model is validated by comparison with experimental results. It is then used to analyze the effect of some operating and design parameters on a constant-pressure sorption process. The adsorbent thickness and heat transfer coefficient between the adsorbent and the heating/cooling fluid have the strongest influence on sorption kinetics and on the cooling capacity of adsorption systems.

1. INTRODUCTION

Adsorption heating and cooling systems have been studied extensively during the last two decades as a serious alternative to vapor compression. Adsorption machines have the advantages of no moving parts, use of other than chlorofluorocarbon refrigerants and can be powered by a low-grade thermal energy source such as waste or solar energy. Adsorption technology is also regarded as a possible solution to cold storage of drugs and food in remote areas, particularly in developing countries.

The present limited development of adsorption systems is due to low efficiencies and the intermittent operation of simple adsorption cycles. A zeolite–water refrigeration cycle has a theoretical coefficient of performance (COP) of about 0.5 [1, 2]. Solar adsorption cooling machines have even lower efficiencies not exceeding 0.1 [3–5]. To overcome these disadvantages, multi-reactor adsorption systems use the principles of heat regeneration to achieve improved performance and continuous operation. Douss *et al.* [6] studied isothermal two and three-reactor adsorption systems and obtained a cooling COP of about 0.7 [7]. Tchernev and Clinch [8] tested a regenerative adsorption cooling system having a COP of 1.2. Hajji and Worek [9] showed that the performance of an ideal regenerative adsorption system can be as high as 1.8.

Proper design of adsorption machines requires good understanding of the simultaneous heat and mass transfer which occur in adsorption reactors. A simple adsorption cycle is composed of two constant-volume and two constant-pressure processes. In a previous work, we studied the constant-volume adsorption process [10]. This paper presents an investigation of adsorption kinetics under constant-pressure conditions. The objective is to develop a theoretical model allowing an accurate analysis of the effect of important operating and design parameters on sorption kinetics and on the behavior of adsorption cooling machines.

In Section 2, the governing equations are derived from the local equilibrium condition and energy balance. Non-linear variations of the physical properties which appear in these equations are discussed in Section 3. The numerical solution and its validation by comparison with known analytical solutions are presented in Section 4. The experimental procedure used to test the theoretical model is described in Section 5. Finally, the influence on adsorption systems of parameters such as the adsorbent thickness, the temperature of regeneration and heat transfer coefficient between adsorbent reactor and the heating/cooling fluid is discussed in Section 6.

2. THEORETICAL ANALYSIS

The adsorbent reactor is supposed to have a rectangular cross-section and a thickness $2E$ much smaller than the length L and the width l. Convective heat transfer occurs between the adsorbent and the heating/cooling fluid on the two largest sides of dimensions $L \times l$ [Fig. 1(a)]. To simplify the analysis, we make the following assumptions: (i) adsorbent temperature and uptake depend only on time and the y-space coordinate—this is valid when the adsorbent thickness is sufficiently small; (ii) the pressure of the vapor phase is uniform through the adsorbent thickness and remains constant; (iii) thermodynamic equilibrium holds at all times—Douss verified in ref. [7] that this assumption is valid when the rate of heat transfer to or from the adsorbent is sufficiently slow; and (iv) the temperature of the heating/cooling fluid is constant.

NOMENCLATURE

$A(W)$	polynomial function introduced in equation (2)
$B(W)$	polynomial function introduced in equation (2)
Bi	Biot number
C	specific heat [J kg^{-1} K^{-1}]
C_{ap}	apparent specific heat [J kg^{-1} K^{-1}]
COP	coefficient of performance
E	half the thickness of adsorbent layer [m]
F	isotherm equation
G	adsorptivity [kg adsorbate (kg adsorbent)$^{-1}$ K^{-1}]
h	heat-transfer coefficient [W m^{-2} K^{-1}]
k	Thermal conductivity [W m^{-1} K^{-1}]
l	width (m)
L	length (m)
$L_v(T)$	heat of vaporization at temperature T [J kg^{-1}]
m, M	mass [kg]
P_v	adsorbate vapor pressure [mbar]
q, Q	heat quantity [W]
r	rate of sorption [kg kg^{-1} s^{-1}]
t	time [s]
T	temperature [°C]
V	volume [m^3]
W	uptake [kg of adsorbate per kg of adsorbent].

Greek symbols

ΔH	heat of sorption [J kg^{-1}]
Δt	time step [s]
Δy	space step [m]
$\Delta\eta$	dimensionless space step
$\Delta\tau$	dimensionless time step
η	dimensionless space coordinate
θ	dimensionless temperature
κ	dimensionless thermal conductivity
ξ	dimensionless apparent specific heat
ρ	density [kg m^{-3}]
τ	dimensionless time
ψ	dimensionless numerical parameter
ω	dimensionless mean uptake.

Subscripts

a	adsorbate
avg	average
con	condensation
cum	cumulative
des	desorbed
equ	equilibrium
eva	evaporation
fin	final
ins	instantaneous
ini	initial
lat	latent heat
s	adsorbent
sen	sensible heat
∞	heating/cooking medium.

2.1. *Governing equations*

The assumption of thermodynamic equilibrium implies that the three state properties T, W and P_v satisfy the isotherm equation

$$\ln(P_v) = F(T, W). \tag{1}$$

For the pair zeolite 4A–water considered in this study, sorption data are fitted well by the following relationship:

$$\ln(P) = A(W) + \frac{B(W)}{T}. \tag{2}$$

$A/(W)$ and $B(W)$ are third-order polynomials with coefficients $A_0 = 14.8979$, $A_1 = 95.4083$, $A_2 = -636.658$, $A_3 = 1848.84$, $B_0 = -7698.85$, $B_1 = 21498.1$, $B_2 = -184598.0$ and $B_3 = 512605.0$ [11]. During a constant-pressure process, the value of the vapor pressure is imposed, therefore the state of the system at position y and time t are determined when the temperature $T(y, t)$ and the uptake $W(y, t)$ are known. The isotherm equation (1) imposes a non-linear relation between T and W having an S-shaped profile. An additional equation is obtained by writing the energy balance of the differential element of thickness Δy shown in Fig. 1(b) between times t and $t+\Delta t$

$$\rho_s(C_s + C_a W)\Delta y \Delta T - \rho_s \Delta y \Delta W \Delta H = \left[\left(k\frac{\partial T}{\partial y}\right)_{y+\Delta y} - \left(k\frac{\partial T}{\partial y}\right)_y\right]\Delta t. \tag{3}$$

The first and second term on the left-hand side correspond to the sensible heats gained by the adsorbent and the adsorbate phase, respectively. The third term is the latent heat of sorption which is proportional to the uptake variation ΔW. The right-hand side terms are the conductive heat fluxes in and out of the differential element. Dividing all terms by $\Delta y\,\Delta t$ and taking the limits $\Delta y \to 0$ and $\Delta t \to 0$ yields:

$$\rho_s(C_s + C_a W)\frac{\partial T}{\partial t} - \rho_s \Delta H \frac{\partial W}{\partial t} = \frac{\partial}{\partial y}\left(k\frac{\partial T}{\partial y}\right). \tag{4}$$

Introducing the 'adsorptivity' $G(T, W)$ and the 'apparent specific heat' C_{ap}, defined as

$$G(W, T) = -\frac{\partial W}{\partial T} \tag{5}$$

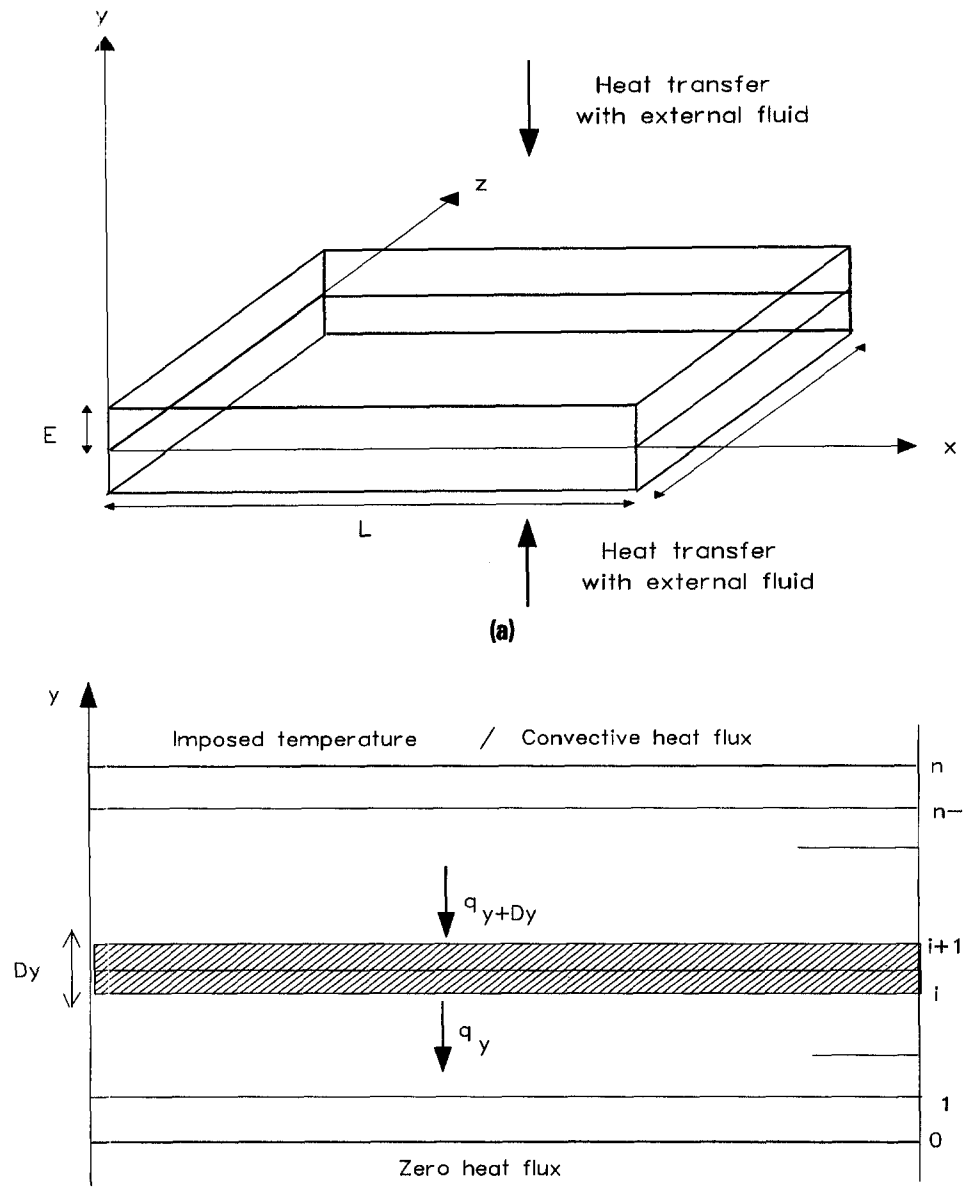

Fig. 1. The adsorbent layer: (a) geometrical dimensions; (b) discretization used in the numerical solution.

$$C_{ap} = C_s + WC_a + G(T, W)\Delta H \tag{6}$$

we obtain a more convenient form of equation (4) as follows:

$$\rho_s C_{ap} \frac{\partial T}{\partial t} = \frac{\partial}{\partial y}\left(k \frac{\partial T}{\partial y}\right). \tag{7}$$

2.2. *Boundary and initial conditions*

At the centre of the adsorbent the symmetry yields adiabatic or zero heat flux condition. At the heat transfer surface, we consider either imposed temperature or convective flux condition. The two solutions should give close results for large heat transfer conditions. Thus:

at $y = 0$:

$$\left(\frac{\partial T}{\partial y}\right)_{y=0} = 0 \tag{8}$$

at $y = E$:

$$T(E, t) = T_\infty \tag{9}$$

or

$$h[T(E,t)-T_\infty] = -k\left(\frac{\partial T}{\partial y}\right)_{y=E}. \quad (10)$$

Uniform temperature and uptake are chosen as initial conditions, thus

$$T(y,0) = T_{ini} \quad W(y,0) = W_{equ}(T_{ini}, P_v). \quad (11)$$

2.3. *System energy analysis*

In order to perform an energy analysis, the following differential heat quantities need to be defined.

Sensible heat gained by the adsorbent:

$$dQ_{sen} = \int_V [\rho_s(C_s + WC_a)\,dT]\,dV. \quad (12)$$

Latent heat of desorption gained by the adsorbent:

$$dQ_{lat} = -\int_V (\rho_s \Delta H\,dW)\,dV. \quad (13)$$

Total heat gained by the adsorbent:

$$dQ_{des} = \int_V (\rho_s C_{ap}\,dT)\,dV = dQ_{sen} + dQ_{lat}. \quad (14)$$

Heat of condensation:

$$dQ_{con} = L(T_{con})\,dm_{des}. \quad (15)$$

Potential cooling effect:

$$dQ_{eva} = [L(T_{eva}) - C_a(T_{con} - T_{eva})]\,dm_{des}. \quad (16)$$

In equations (15) and (16), dm_{des} is the desorbed mass between t and $t+dt$.

Corresponding cumulative heat quantities are obtained by integrating the above expressions between times 0 and t. The performance of an adsorption cooling cycle is expressed by the ratio of the potential cooling effect to the total heat of desorption. Instantaneous and cumulative values of this ratio define the following coefficients of performance:

$$COP_{ins}(t) = \frac{[L - C_a(T_{con} - T_{eva})]\,dm_{des}(t)}{\int_V (\rho_s C_{ap}\,dT)\,dV} \quad (17)$$

$$COP_{cum}(t) = \frac{[L - C_a(T_{con} - T_{eva})]m_{des}(t)}{\int_{T_{ini}}^{T(t)} \left(\int_V \rho_s C_{ap}\,dV\right) dT}. \quad (18)$$

2.4. *The rate of sorption*

For a non-uniform uptake distribution, the mass of the adsorbed phase at time t is obtained by integrating the uptake W over the volume of the adsorbent

$$M_a(t) = \rho_s \int_V W\,dV. \quad (19)$$

Introducing the average uptake $W_{avg}(t)$ defined as

$$W_{avg}(t) = \frac{1}{V}\int_V W\,dV. \quad (20)$$

the expression of $M_a(t)$ becomes

$$M_a(t) = M_s W_{avg}(t). \quad (21)$$

Since the desorbed mass $m_{des}(t)$ between times 0 and t is equal to the change in the mass of the adsorbed phase, we have

$$m_{des}(t) = M_a(0) - M_a(t) = M_s[W_{ini} - W_{avg}(t)]. \quad (22)$$

As the final equilibrium state characterized by uniform temperature T_∞ and uptake W_{fin} is approached, the desorbed mass tends to its maximum value $m_{des}(\infty)$ given by

$$m_{des}(\infty) = M_a(0) - M_a(\infty) = M_s(W_{ini} - W_{fin}). \quad (23)$$

The progress of the desorption process can be measured by the ratio

$$\omega(t) = \frac{m_{des}(t)}{m_{des}(\infty)} = \frac{W_{ini} - W_{avg}(t)}{W_{ini} - W_{fin}} \quad (24)$$

which is a dimensionless average uptake between zero and unity and proportional to the desorbed mass. The rate of sorption $r_{des}(t)$ is defined as the mass flow of desorbed mass per unit adsorbent mass, expressed by

$$r_{des}(t) = \frac{1}{m_{des}(\infty)}\frac{dm_{des}(t)}{dt} = \frac{d\omega(t)}{dt}. \quad (25)$$

3. VARIATIONS OF THE ADSORPTIVITY AND THE APPARENT SPECIFIC HEAT

Introducing the apparent specific heat simplified the form of the governing equations. In order to avoid convergence and stability problems in the numerical solution, it is necessary to show the variations of C_{ap} with the temperature and uptake. Using equation (2), the expression of the adsorptivity for a constant-pressure process is straightforward:

$$G(W,T) = \frac{B(W)}{T^2 A'(W) + TB'(W)}. \quad (26)$$

$A'(W)$ and B[ssp](W) are the first derivatives of $A(W)$ and $B(W)$ with respect to W. Figure 2 shows the variations of C_{ap} with temperature and uptake for various condensation temperatures. G presents a similar behavior of bell-shaped curves due to the predominance of latent heat of sorption compared with sensible heat. As an example, for a condensing temperature of 30°C, G varies from 5 to 25×10^{-4} kg kg^{-1} K^{-1} with a maximum value reached at 140°C. C_{ap} increases from 4 kJ kg^{-1} K^{-1} at 20°C to a maximum value of 9.2 kJ kg^{-1} K^{-1} at 135°C. Maximum values of G and C_{ap} occur at an uptake of about 12%.

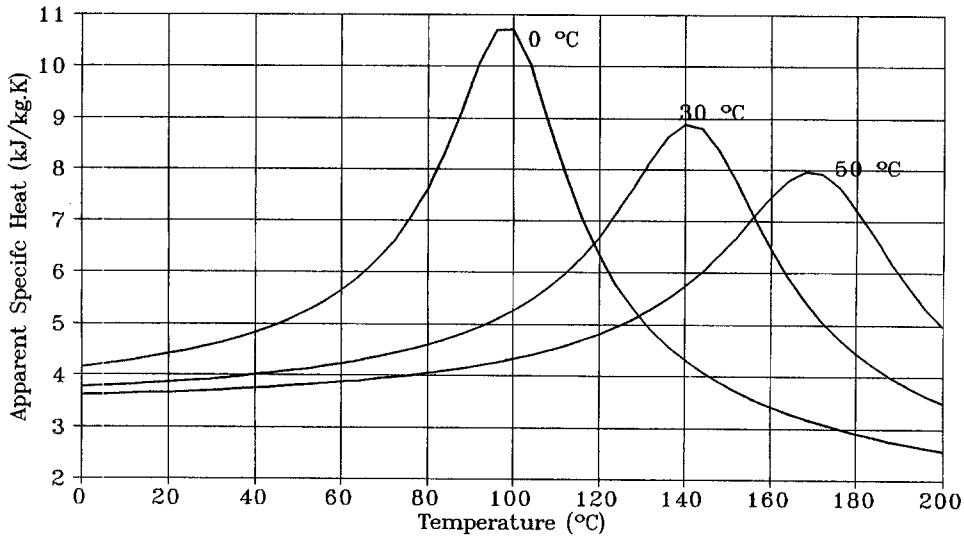

(a)

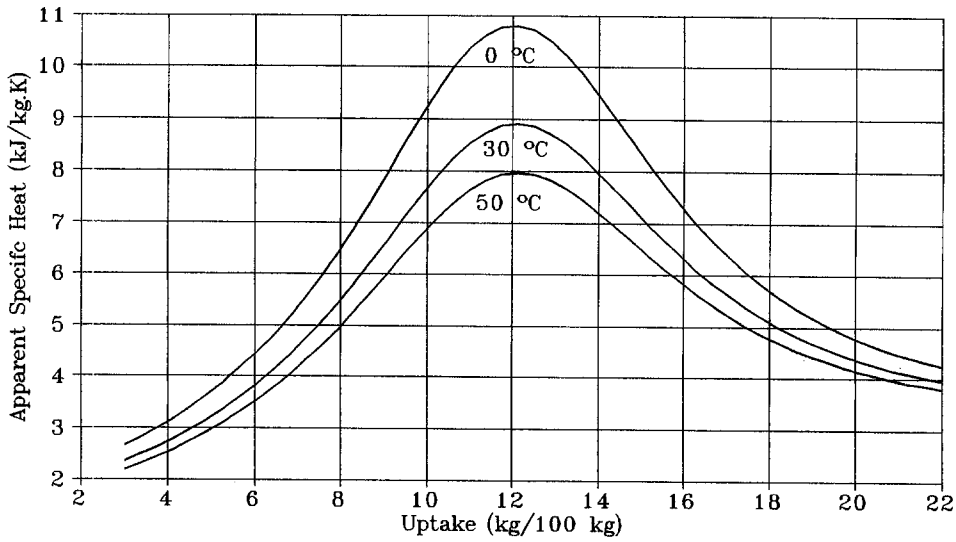

(b)

Fig. 2. Variations of the apparent specific heat with: (a) the temperature; (b) the uptake.

4. NUMERICAL SOLUTION

4.1. *Finite difference equations*

To obtain a finite difference form of the governing equations, the adsorbent thickness is divided into n elements of thickness Δy [Fig. 1(b)]. An energy balance is written for each element between times t and $t+\Delta t$. During this period, the physical properties of each element are considered to be constant. By introducing the following variables and parameters

$$\eta = \frac{y}{E} \quad \tau = \frac{k_s t}{\rho_s C_s E^2} \quad \theta = \frac{T - T_\infty}{T_{ini} - T_\infty}$$
$$\xi = \frac{C_{ap}}{C_s} \quad \kappa = \frac{k}{k_s} \tag{27}$$

$$Bi = \frac{hE}{k} \quad \Delta\eta = \frac{1}{n-1} \quad \Delta\tau = \frac{k_s \Delta t}{\rho_s C_s E^2} \quad \psi = \frac{\Delta\tau}{(\Delta\eta)^2} \tag{28}$$

a convenient dimensionless form of the explicit finite difference equations is obtained as follows.

For $j = 1$:

$$\theta_1^{p+1} = \frac{2\psi\kappa_1^p}{\xi_1^p}\theta_2^p + \left[1 - \frac{2\psi\kappa_1^p}{\xi_1^p}\right]\theta_1^p. \tag{29}$$

For $1 < j < n$:

$$\theta_j^{p+1} = \frac{\psi\kappa_j^p}{\xi_j^p}[\theta_{j+1}^p + \theta_{j-1}^p] + \left[1 - \frac{2\psi\kappa_j^p}{\xi_j^p}\right]\theta_j^p. \quad (30)$$

For $j = n$:

case of imposed temperature

$$\theta_n^{p+1} = 0 \quad (31)$$

case of convective heat transfer

$$\theta_n^{p+1} = \frac{2\psi\kappa_n^p}{\xi_n^p}\theta_{n-1}^p + \left[1 - \frac{2\psi(\kappa_n^p + Bi\,\Delta\eta}{\xi_n^p}\right]\theta_n^p. \quad (32)$$

To avoid instability of the numerical solution, we make sure that the coefficients are positive by imposing on time and space steps the following conditions:

case of imposed temperature

$$1 - \frac{2\Delta\tau\kappa_j^p}{(\Delta\eta)^2\xi_j^p} \geqslant 0 \quad (33)$$

case of convective heat transfer

$$1 - \frac{2\Delta\tau}{(\Delta\eta)^2\xi_n^p}[\kappa_n^p + Bi\,\Delta\eta] \geqslant 0. \quad (34)$$

For a specified space increment, the time step is determined from the above conditions as follows:

case of imposed temperatures

$$\Delta\tau \leqslant \frac{(\Delta\eta)^2 \min(\xi_j^p)}{2\max(\kappa_j^p)} \quad (35)$$

case of convective heat transfer

$$\Delta\tau \leqslant \frac{(\Delta\eta)^2 \min(\xi_n^p)}{2[\max(\kappa_n^p) + Bi\,\Delta\eta]}. \quad (36)$$

A computer program has been developed based on this numerical scheme. The program calculates, for each value of time, the spatial temperature and uptake distributions as well as their average values. It also calculates instantaneous and cumulative values of the desorbed/adsorbed mass, the energy quantities defined previously and the system coefficients of performance. The specific heat and thermal conductivity of the adsorbent–adsorbate mixture are considered as linear functions of the uptake but the numerical scheme can be readily used with more complex expressions involving eventually temperature-dependent terms.

4.2. *Validation of the numerical solution*

If the apparent specific heat and thermal conductivity are assumed to be constant, the governing equations reduce to the classical problem of transient heat conduction in a slab of which we have an exact solution in terms of a Fourier series [12]. Therefore, the numerical solution can be validated by comparing the temperature profile calculated by the computer program with that obtained from the analytical expression using the mean values of the apparent specific heat and thermal conductivity. Figure 3 shows that the maximum difference between the two profiles does not exceed 5%. The data used to obtain this figure are given in the following section and the mean values of the apparent specific heat and thermal conductivity are 6.6 kJ kg^{-1} K^{-1} and 0.4 W m^{-1} K^{-1}, respectively.

5. COMPARISON WITH EXPERIMENTAL RESULTS

Figure 4 shows the apparatus used in this study. The adsorbent sample is enclosed in a tight copper box immersed in a thermostatic bath. The box is connected to a scaled tube which collects the condensing adsorbate. The tube is cooled by an external water loop. The pressure of the gas phase and the bath temperature are recorded using a data logger. Starting from an equilibrium state defined by the adsorbent temperature T_i and vapor pressure, the sample temperature is changed to a second equilibrium state at the temperature T_∞ of the heating/cooling fluid while maintaining the vapor pressure constant by the cooling water loop.

Typical test data are: copper box dimensions, 12×6 mm; adsorbent thickness, $2E = 8$ mm; mass of adsorbent, 59.1 g; initial temperature, $T_{ini} = 20°C$; heating fluid temperature, $T_\infty = 150°C$; heat transfer coefficient $h = 30$ W m^{-2} K^{-1}; and condensing temperature, $T_{con} = 20°C$. Using thermal properties of the zeolite–water pair given in Table 1 leads to a characteristic time of 16.38 s and a Biot number equal to 0.6. A numerical solution is obtained by taking a dimensionless space step of 0.2 ($n = 6$). It is noticed that a smaller step does not improve the accuracy. The stability condition imposes a maximum time step of 6.41×10^{-3} so we chose $\Delta\eta = 0.006$. With these values, the calculated and measured profiles of the desorbed mass are very close (Fig. 5).

Agreement with experimental data indicates that the present one-dimensional model gives reasonably accurate results when the thickness is about six times smaller than the dimensions of the heat transfer area. This is also confirmed by a two-dimensional model developed later in order to analyze the improvement of sorption kinetics by inserting metallic fins in the adsorbent material [13].

6. RESULTS AND DISCUSSION OF THE PARAMETRIC STUDY

After its validation, the model developed here is used to analyze the behavior of sorption systems and the effect of some operating and design parameters on sorption kinetics and on cooling capacity. Both parameters are directly related to the machine size as faster sorption and higher cooling capacity means lighter and competitive machines. Zeolite 4A–water is

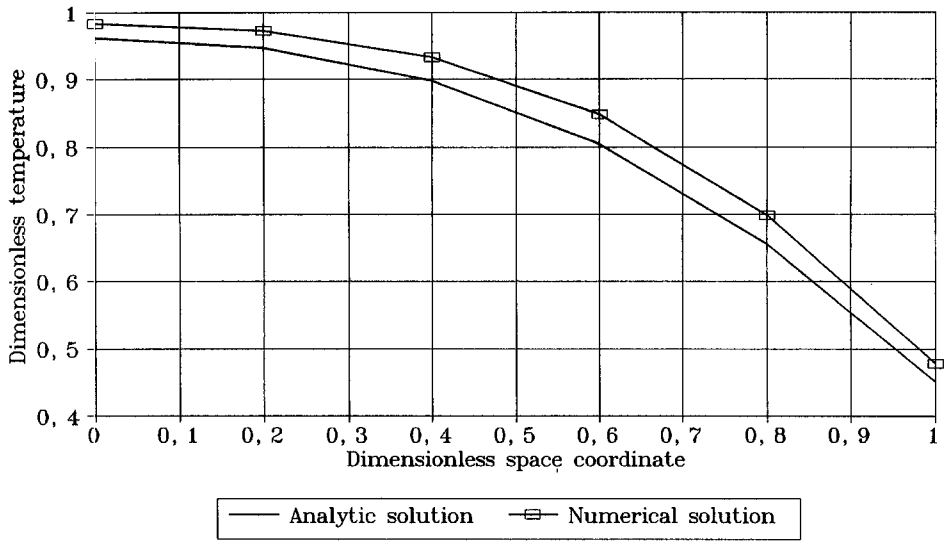

Fig. 3. Comparison of the numerical solution with the analytical solution of transient heat transfer in a slab with imposed surface temperature.

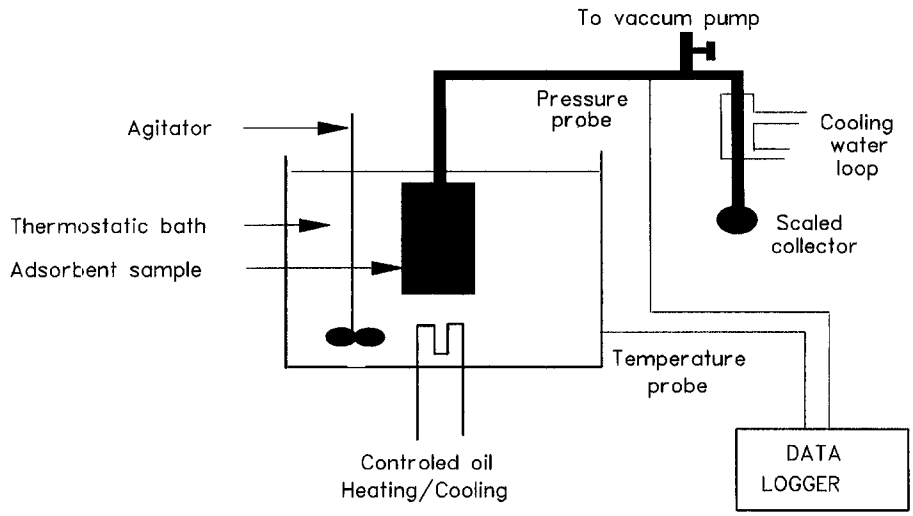

Fig. 4. Schematic of the experimental setup.

chosen as the working pair. The data used in the parametric study are summarized in Table 1. The analysis includes the effect of the adsorbent thickness, the heat transfer coefficient, the difference between initial and final adsorbent temperatures and the temperature of condensation.

Figure 6 shows that the rate of desorption decreases with time and tends to zero. As a consequence the mass of desorbed species increases rapidly at the beginning of the process before reaching its asymptotic value. This behavior is due to the fact that adsorbate becomes more and more difficult to extract when the uptake decreases. Energy quantities which are essentially proportional to the desorbed mass present similar trends. The latent heat accounts on average for 66% of the total energy of desorption. The heat of condensation represents 51% of the heat of desorption. We also see that the instantaneous COP reaches a maximum value of 0.57. This behavior and the cycle cumulative COP of about 0.5 are in agreement with published data [2, 5].

The adsorbent thickness which appears in the expression for dimensionless time and Biot number, has a strong influence on sorption kinetics. The desorption process is almost finished at $\tau = 4.7$ (6 min for $E = 5$ mm) while its progress does not exceed 15% at $\tau = 0.13$ (same 6 min period for $E = 30$ mm). Similarly, for a 5 min desorption time, the cooling capacity is doubled when the thickness is reduced from 10 to 5 mm (τ increases from 1 to 4).

Table 1. Elements of the parametric study

Parameter	Value
Adsorbent:	
Nature	Zeolite-4A
Mass density [kg m^{-3}]	735
Specific heat [J kg^{-1} K^{-1}]	836
Thermal conductivity [W K^{-1} m^{-1}]	0.2
Thickness [m]	0.010/variable
Adsorbate:	
Nature	Water
Specific heat [J kg^{-1} K^{-1}]	4180
Thermal conductivity [W K^{-1} m^{-1}]	0.6
Operating conditions:	
Condensation temperature [°C]	37.8/variable
Heating fluid temperature [°C]	200/variable
Initial temperature [°C]	20/variable
Heat transfer coefficient [W m^{-2} K^{-1}]	500/variable

The heat transfer coefficient which appears in the expression for the Biot number also has a marked influence on sorption kinetics (Fig. 7). For $Bi = 25$ ($h = 500$ W K^{-1} m^{-2}), the desorption process is finished at $\tau = 5.9$ (30 min) while only 80% of desorption is achieved during the same period for $Bi = 2.5$ ($h = 50$ W K^{-1} m^{-2}). The cooling capacity changes in the same proportions. No improvement is expected by increasing the Biot number beyond 25.

The difference between hot and cold temperatures has relatively little effect on sorption kinetics (Fig. 8); however, it affects considerably the cooling capacity as the latter is doubled when the temperature difference increases by 50°C. This is explained by the increase in uptake variation resulting from an important difference between hot and cold temperatures. With the zeolite 4A–water pair, uptake variation increases from 15.8 g kg^{-1} between 20 and 50°C to 50.3 g kg^{-1} between 20 and 100°C and 172 g kg^{-1} between 20 and 200°C.

The condensation temperature which imposes the vapor pressure in the adsorbent reactor has little effect on sorption kinetics although a reduction of the condensation pressure speeds up the desorption process (Fig. 9); however, the cooling capacity increases by about 40% when condensation occurs at 20°C instead of 40°C, again as a result of uptake variation.

7. CONCLUSIONS

A theoretical model is developed to study sorption kinetics and the behavior of adsorption cooling systems during a constant-pressure adsorption process. The non-linear governing equations are solved numerically and the solution compares well with known analytical expressions. An experimental study is also conducted in order to test the model. The comparison revealed a very good agreement between model predictions and experimental data.

The model is then used to evaluate the influence of various important design and operating parameters on sorption kinetics and on the performance of adsorption cooling machines. The parametric investigation shows that the adsorbent thickness and heat transfer coefficient have major effects on sorption kinetics. The cooling capacity of sorption systems can be substantially increased by using thinner adsorbent layers and enhancing heat transfer rates. The condensation temperature and the adsorbent temperature difference between initial and final states also have a non-negligible influence. Faster operation requires operating at lower condensing temperature and a bigger difference between cold and hot adsorbent temperatures.

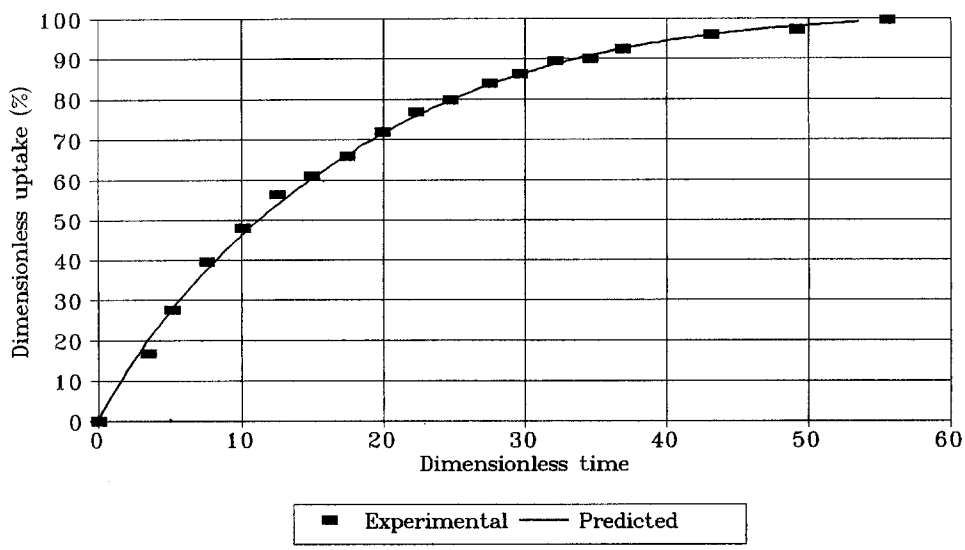

Fig. 5. Measured and calculated values of the mean dimensionless uptake.

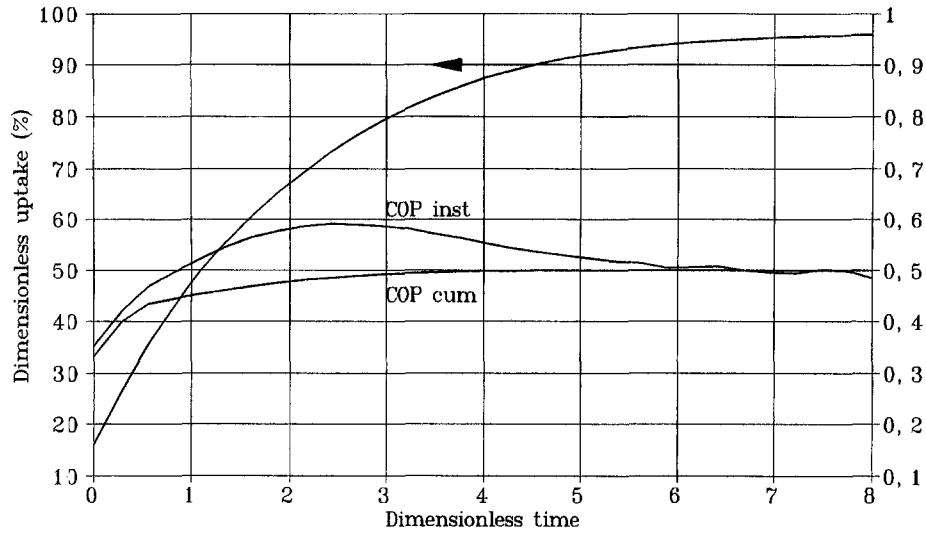

Fig. 6. Profiles of the mean dimensionless uptake and the instantaneous and cumulative COPs ($Bi = 25$).

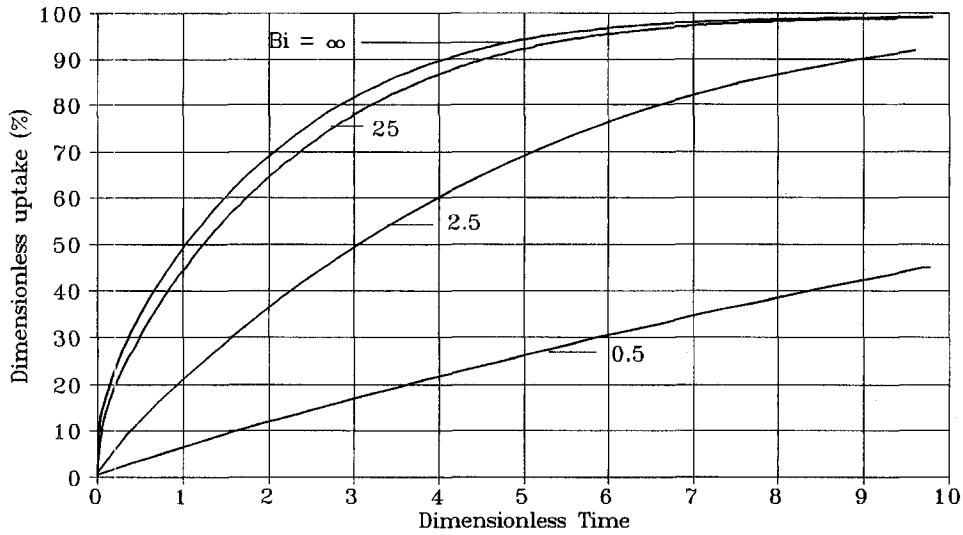

Fig. 7. Effect of the heat transfer coefficient on sorption kinetics ($Bi = 25$).

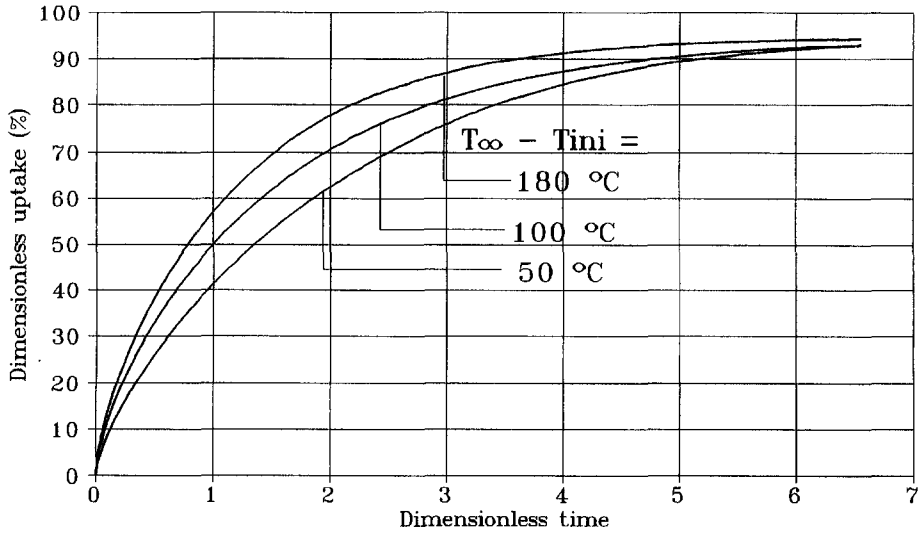

Fig. 8. Effect of the temperature difference ($T_\infty - T_{ini}$) on sorption kinetics ($Bi = 25$).

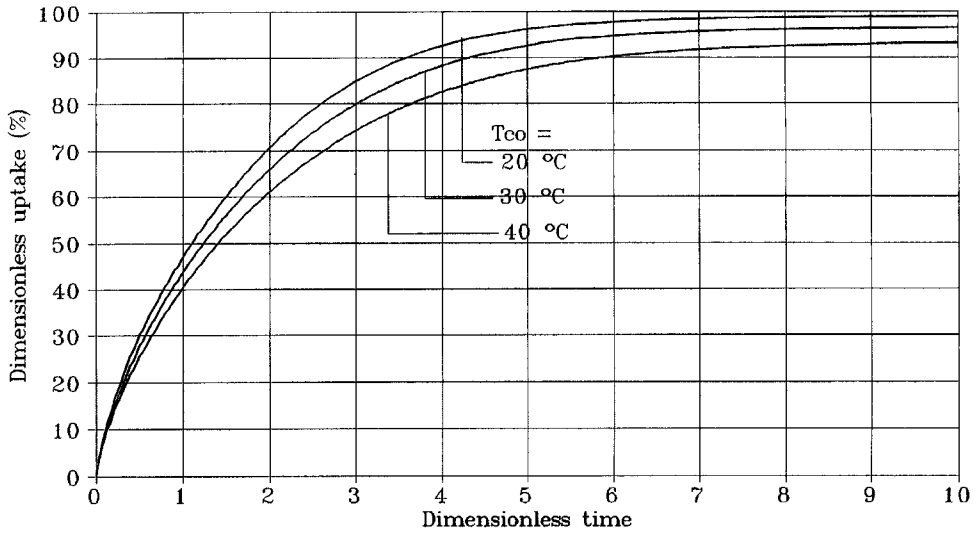

Fig. 9. Effect of the condensation temperature on sorption kinetics ($Bi = 25$).

REFERENCES

1. D. I. Tchernev, *Zeolites and Clay Minerals as Sorbents and Molecular Sieves* (Edited by L. B. Sand and F. A. Mumpton), pp. 479–484. Academic Press, New York (1979).
2. J.-J. Guilleminot, F. Meunier and B. Mischler, Etude des cycles intermittents à adsorption solide pour la réfrigération solaire, *Rev. Phys. Appl.* **15,** 441–452 (1980).
3. R. E. Critoph and R. Vogel, Possible adsorption pairs for use in solar cooling, *Int. J. Ambient Energy* **7,** 659–667 (1986).
4. R. E. Critoph, Performance limitation of adsorption cycles for solar cooling, *Sol. Energy* **41,** 21–31 (1988).
5. A. Hajji, W. M. Worek and Z. Lavan, Dynamic analysis of a closed-cycle solar adsorption refrigerator using two adsorbent–adsorbate pairs, *ASME J. Sol. Energy Engng* **113,** 73–79 (1991).
6. N. Douss, F. E. Meunier and L. M. Sun, Predictive model and experimental results for a two-adsorber solid adsorption heat pump, *Ind. Engng Chem. Res.* **27,** 310–316 (1988).
7. N. Douss, Etude expérimentale de cycles à cascades à adsorption solide, Ph.D. Thesis, Orsay, France (1988).
8. D. I. Tchernev and J. M. Clinch, Closed-cycle zeolite regenerative heat pump, *Proceedings of the Eleventh Annual ASME Solar Energy Conference*, pp. 347–351 ASME, New York (1989).
9. A. Hajii and W. M. Worek, Simulation of a regenerative closed-cycle adsorption cooling/heating system, *Energy* **16,** 643–654 (1991).
10. A. Hajii, G. Cacciola and G. Restuccia, Experimental and theoretical study of a constant-volume adsorption process, *Energy* **19,** 961–965 (1994).
11. G. Cacciola, A. Hajji, G. Maggio and G. Restuccia, Dynamic simulation of a recuperative adsorption heat pump, *Energy* **18,** 1125–1137 (1993).
12. F. P. Incropera and D. P. De Witt, *Introduction to Heat Transfer*, Chap. 5. Wiley, New York (1985).
13. S. Khalloufi, Modélisation des transferts de chaleur et de matière dans les machines frigorifiques et les pompes à chaleur à adsorption. Mémoire de fin d'Etudes, Institut Agronomique Hassan II, Rabat (1993).